Image-based Deep Learning on Air Quality Using A 9-Layer Residual Neural Network

Amy Yang

Table of Contents

List of Figures and Tables

Image-based Deep Learning on Air Quality Using A 9-Layer Residual Neural Network

Amy Yang

Abstract

The increasing prominence of air pollution has continued to negatively impact humans and the planet in various ways, ranging from respiratory and cardiovascular diseases to the damage of crops and the creation of severe weather. Air quality monitoring systems are essential tools that allow for a deepened understanding of air pollution and its influence on people and places. However, many monitors around the world are outdated, broken, or simply don't exist, as a result of high costs and sophistication. In this study, air quality was analyzed by estimating air pollution from various natural images, focusing on levels of particulate matter (PM2.5), a common pollutant with a diameter of less than 2.5 micrometers. The Residual Neural Network (ResNet9), a machine learning model, was used to classify 862 images into three classes of PM2.5 concentrations: Good (<35.4μg/m³), Unhealthy (35.5~150.4μg/m³), and Hazardous (>150.5μg/m³). To perform this classification, a combined dataset was created with webcam images from Beijing and Yosemite National Park, and their corresponding levels of PM2.5. After training and testing the model, the results showed optimal performance of the ResNet9 model, therefore validating this method of PM2.5 concentration estimation. The model achieved an average accuracy of 83% compared to 69% by current state-of-the-art models. This model provides cost-effective and efficient air quality monitoring for individuals and governmental organizations, which can immensely benefit human health and reduce air pollution.

Introduction

Overview

In 2021, the World Health Organization declared climate change to be the "single biggest health threat facing humanity." The amalgam of air pollution from natural sources (ex. wildfires) and human sources (ex. vehicle emissions) greatly contribute to the heightened problem of climate change. Air pollution has risen tremendously in the past years and remains problematic as urbanization and industrialization rapidly increase (Chen et al., 2017). Many different sectors, such as tourism, energy, and agriculture generate immense amounts of pollution, thus perpetuating global warming and natural disasters (Lenzen et al., 2018). Pollution is also detrimental to living organisms, killing around 7 million people yearly from the effects of air pollution worldwide (Kortoci et al., 2022). Greater efforts need to be made to address the dangers of air pollution in various environments, ranging from cities to national parks. As technology advances, this problem can now be alleviated using image processing models, which have the potential to detect air quality levels through real-time photos.

Review of Literature

Air Quality Monitors in National Parks

The Environmental Protection Agency (EPA) is a public health agency mainly focused on the protection of the environment and public health (McCarthy et al., 2017). In 2017, the EPA amended the Regional Haze Rule, which required states to reduce pollution from large industrial sources that contribute to haze in 90% of all national parks and wilderness areas. States were given an extension until July 31st, 2021, to complete their plans. Despite this, 15 states were put on notice in August 2022, after failing to submit Regional Haze Plans. In response to the EPA's failure to enforce this law, Stephanie Kodish, Senior Director and Counsel for National Parks Conservation Association's (NPCA) Clean Air and Climate Programs, said in a statement, "Nearly every national park is affected by air pollution, harming our parks' waters, wildlife and landscapes, and threatening the health of millions of park visitors and vulnerable communities across the county." There are significant shortcomings in the understanding of air pollution in our national parks. According to a report by the NPCA, 69 national parks have air quality monitors outside their boundaries, 230 have monitors inside their boundaries, and 124 have no air monitors at all. Many monitors are outdated and broken, providing inadequate data regarding air quality. Similarly, in many other countries, air quality monitors are not readily available, due to the expensive set-up cost and sophisticated sensors.

Particulate Matter

Air pollution occurs when the atmosphere is contaminated with excessive and harmful substances. These substances include gasses, particulates, and biological molecules. Pollutants can be further classified into primary and secondary pollutants. Primary pollutants are emitted directly from the source to the atmosphere. Common examples include sulfur dioxide (SO2), particulate matter (PM), nitrogen oxide (NOx), and carbon monoxide (CO). The latter classification, secondary pollutants, results from the chemical or physical interactions between primary pollutants. Some examples include photochemical oxidants and secondary particulate matter. These excessive pollutants are detrimental to the human population and the environment because they cause disease, impair crops, and kill living organisms (Eusébio et al., 2021). In particular, fine particulate matter, PM2.5 (particles with a diameter less than 2.5 micrometers), can cause harmful respiratory effects by penetrating the lung and corroding the alveolar wall, hence impairing lung function (Xing et al., 2016). Furthermore, increased exposure to PM2.5 can cause cardiovascular risks, such as heart attacks and strokes. When comparing PM2.5 to PM10 (particles with a diameter greater than 2.5 micrometers), PM10 does not remain airborne as long and their spatial impact is usually limited since they typically deposit on the ground. Unlike PM2.5, PM10 cannot be readily transported across broader areas because they are generally too large to remain suspended in the air. Rather, PM2.5 remains airborne for long periods and travels hundreds of miles. Not only does PM2.5 cause environmental and health damage, but these particles also impair visibility.

Deep Learning

Visibility in the atmosphere is a crucial factor in determining air quality. With the widespread advancement of technology in the past decades, capturing photos has increased availability and played a significant role in representing and describing information (Chakma et al., 2017). Using tools such as deep learning, images can be classified into various categories based on target factors. In the instance of analyzing air quality, image classification has the potential to connect individuals (ex. a smartphone user) directly with an estimation of real-time air quality by simply taking a picture of their

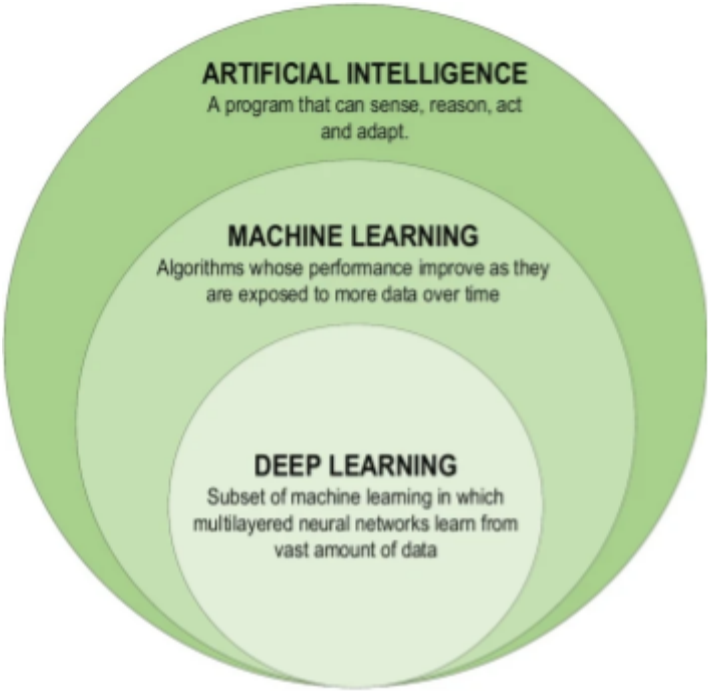

Figure 1: Artificial intelligence, machine learning, and deep learning diagram. Diagram displays deep learning as a subset of both machine learning and artificial intelligence. Layers are confined within another to distinguish certain features. (Alzubaidi et al., 2021)

surrounding environment. In areas with high concentrations of PM2.5, the air appears hazy and visibility decreases. Real-time climate/weather images could capture these fluctuations in the atmosphere and partnered with machine learning, these photos can be classified into air quality metrics, such as PM2.5 levels. This would develop an efficient and affordable method of monitoring air quality.

Artificial intelligence is a computer system that mimics human intelligence to perform tasks. Machine learning, a subset of artificial intelligence, uses mathematical models to help computers learn and improve upon their ability to accomplish given tasks by gathering information. As seen in Figure 1, deep learning, a subfield of both machine learning and artificial intelligence, is especially applicable when mapping given inputs to their corresponding labels in large datasets (Alzubaidi et al., 2021). Within deep learning, neural networks are a series of algorithms that mimic the human brain by detecting patterns and

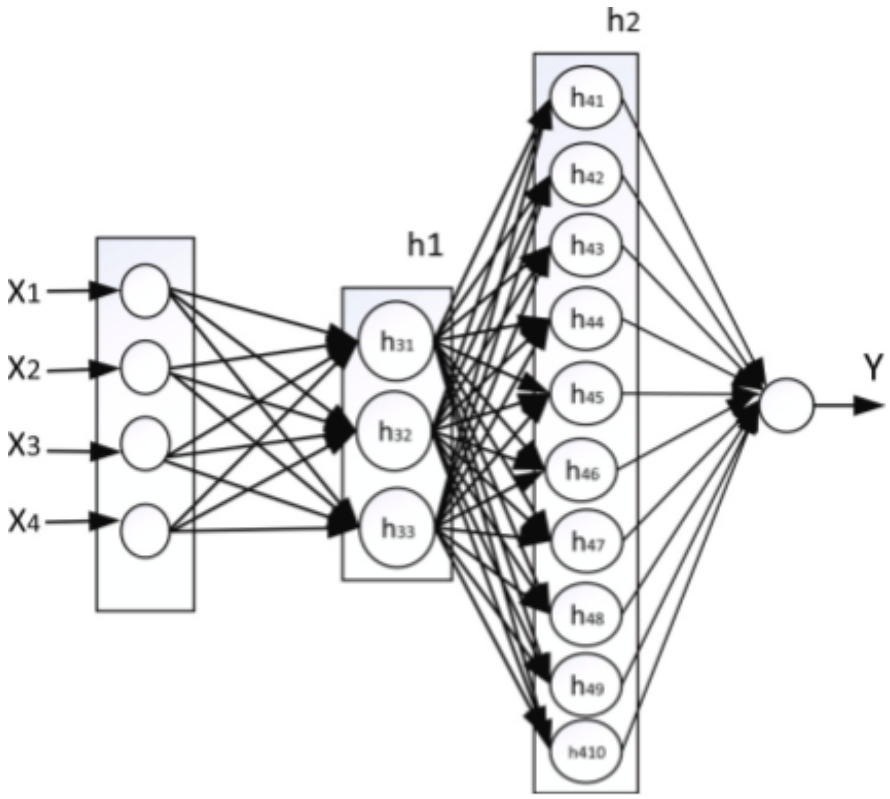

Figure 2: Visual model of a deep neural network consisting of an input layer with four inputs (x_1, x_2, x_3, x_4), two hidden layers (h1, h2), and an output layer (Y). Each layer contains neurons (ex. h_{31}, h_{32}, h_{33}) which are connected to previous and following layers. At each connection adjoining neurons, weights and biases are adjusted to optimize the neural network. (Rachmatullah et al., 2021)

making comparisons to the general pattern (Sadiq et al., 2019).

Neural networks are constructed from three types of layers: input, hidden, and output (Xing et al., 2019). The input layer consists of the initial raw data and the output layer produces results for the given

inputs. Between these two layers is the hidden layer, where all the computation is done. This type of layer often contains many layers, each trying to learn a new aspect of the data by minimizing the error (Figure 2). Additionally, every layer contains many neurons, and each connection between neurons -- referred to as the synapse -- has an associated weight (Koutsoukas et al., 2017). This weight helps determine how much an input will influence the output. Initially, a neural network is assigned a set of weights when it is trained on the training set. During the network's training period, the weights are optimized by adjusting parameters to maximize the model's performance (Rachmatullah et al., 2021). Further, a bias is introduced to reduce variance in the output and produce better generalization of the neural network. The bias is a constant value that is added to the product of the weight and input. Ultimately, the neural network output function is as follows:

$$Y = \sum (weight * input) + bias$$

Firstly, a neuron will compute the weighted sum of the inputs. Then, a constant value of bias is added. Finally, a computed value is fed into the function, which will yield an output.

Residual Network

A commonly used neural network is the Residual Network (ResNet) which is widely used for image and object classification. ResNet can train hundreds or thousands of layers and still achieve compelling performance (He et al., 2015). Previous studies have leveraged methods of deep learning (ex. Convolutional Neural Network and Random Forest Classifier) to develop air quality monitoring systems. However, accuracy rates were relatively low and results were unable to be generalized due to limited training data. In this study, the first method of air quality analysis using a ResNet model is conducted with an emphasis on national parks.

Statement of Purpose

Problem Statement

1. The reluctance of national parks and states to implement air quality monitors paired with the costly set-up and sophistication of these monitors results in the shortage of monitors in areas where they are crucially needed.
2. Previous deep learning monitoring systems perform with low accuracy and have a limited variety of training images.

Objective

1. Build, train, and test an image-based ResNet deep learning model which will classify images based on their PM2.5 concentration level. Determine if the model is a valid method of estimating PM2.5 levels and if the model can be recommended for future air quality detection as an alternative to expensive air quality sensors.
2. Create a dataset containing images from diverse geographic locations (Beijing and Yosemite National Park), and integrate values of PM2.5 concentrations in correspondence with the location and time of each obtained photo.

Hypothesis

1. The ResNet model is an accurate and valid deep learning model for the detection of air pollution. Compared to previous deep learning models, the ResNet model will produce greater accuracy rates, because new releases of Python come with bug fixes and new features. Also, the ResNet framework is better suited for the given task of estimating PM2.5 concentration levels over other deep learning methods.
2. The ResNet model is more highly favored over previous deep learning models, such as the Convolutional Neural Network and the Random Forest Classifier, as ResNet is trained with a larger image dataset with greater variations of environments (ex. urban, rural, etc).

Methodology

From my mentor, assistance was provided in establishing background knowledge in the field of machine learning through research literature to understand prior work. Machine learning platforms such as PyTorch and Keras were suggested in the progression of the research. Additionally, feedback was given on the experiments and research report. Help from my mentor allowed me to understand the fundamentals of machine learning and specifically how to build, train, and test a neural network.

ResNet9

Since the ground-breaking ResNet model was created in 2015, the field of deep learning has advanced immensely. The performance of computer vision tasks such as image, object, and face recognition has been boosted. In comparison to other Convolutional Neural Networks (CNN) such as GoogleNet, containing 22 convolutional layers, this ResNet contained 9 convolutional layers (ResNet9). This model used the ResNet9 framework to combat the vanishing gradient problem in very deep CNNs. The vanishing gradient problem occurs when more layers are added to a neural network and the derivatives of the loss function approach zero, which makes the neural network more difficult to train. The loss function refers to an evaluation of how well the model can predict expected outcomes. By

skipping some network layers in the ResNet9 model, this machine learning framework would ultimately generate better model performance.

Dataset

Since there was no publicly available PM2.5 concentration image dataset, a dataset was created using 862 images. Of these images, 456 were obtained from a Beijing tourist website, which contained archives of real-time weather photos, including descriptions of the date, time, and location of each image. A variety of images were taken under diverse weather conditions and seasons from a 7-year timeframe: 2014 - 2021. The remaining 406 images were collected from the National Park Service's Yosemite webcam. This webcam contains archives of weather images taken from the Turtleback Dome within Yosemite National Park. Similarly, these images were taken from 2014 - 2021. Beijing and Yosemite were chosen based on the variety and fluctuation of air quality levels extended over many years. Additionally, the local Beijing tourist site and the National Parks Service (NPS) both had a wide range of accessible webcams and weather photos. In the random selection of 128 photos as seen in Figure 3, the Beijing and Yosemite National Park datasets display various levels of PM2.5. Each image from this combined dataset contains a sky region and different objects with various depths to allow for the detection of air quality levels. PM2.5 levels were extracted from the AirNow database, which contains ozone, PM2.5, and PM10 levels from areas around the world with functioning air quality monitors. PM2.5 levels were correspondingly associated with the location and date of each image. PM2.5 concentrations were separated into three classes: Good (<35.4μg/m³), Unhealthy (35.5~150.4μg/m³), and Hazardous (>150.5μg/m³).

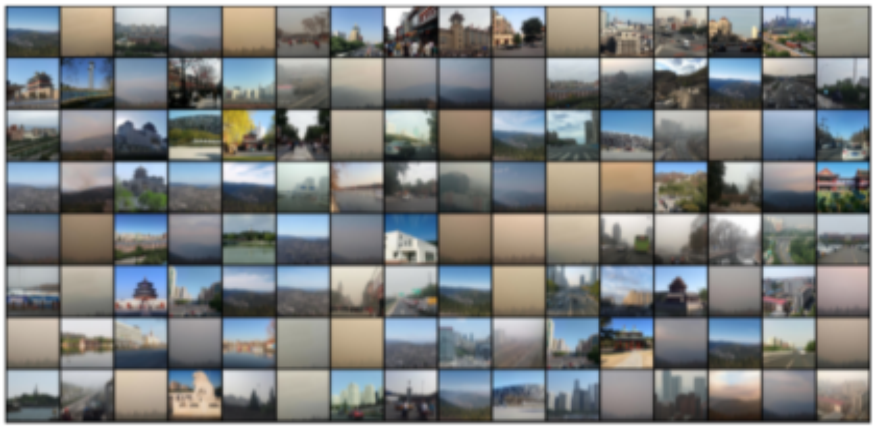

Figure 3: Random batch size selection of 128 photos taken from both Beijing and Yosemite National Park datasets from 2014 - 2021, each displaying various levels of PM2.5 that were then separated into three classes: Good (<35.4μg/m³), Unhealthy (35.5~150.4μg/m³), and Hazardous (>150.5μg/m³).

Training and Testing

To train the ResNet9 model, 90% of the images were randomly selected and included in the training dataset and the remaining 10% were used for the validation dataset. Each image resolution was 320 x 213 pixels but was later rescaled to 64 x 64 pixels to fit the input size of the first ResNet9 layer.

Figure 4 shows an image from the Beijing dataset with Good (<35.4µg/m³) PM2.5 levels before rescaling (left image) and the same image after scaling to 64 x 64 pixels (right image).

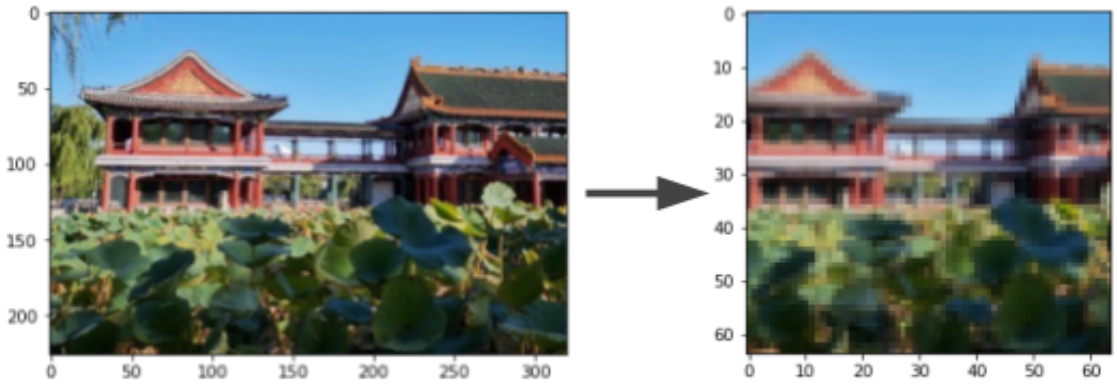

Figure 4: Rescaling images to 64 x 64 pixels. The image on the left displays a 320 x 213 photo from the Beijing dataset with Good (<35.4µg/m³) levels of PM2.5 concentration before rescaling. The image on the right is the same photo after rescaling to 64 x 64 to fit the first ResNet9 input layer.

Hyperparameters

Hyperparameters were adjusted to produce an optimal performance of the model. After training and testing the model on the training and validation sets, the observed model performance allowed for the tuning of hyperparameters to control the learning process and determine a set of values that maximized the model's performance and minimized errors. The hyperparameters used in this model include model architecture, batch size, epochs, learning rates, and optimization algorithm. In neural networks, the model architecture consists of the number of network layers, the number of neurons per layer, and the activation function, which defines the output of a neuron given an input or set of inputs. The batch size is a hyperparameter that refers to the number of samples that will be passed through the network in one run. Epochs are the number of iterations an algorithm takes around a training dataset. Additionally, learning

Table 1: Hyperparameters on the ResNet9 model, including architecture type, batch size, epochs, learning rates, and the optimization algorithm.

Hyperparameters 1s

arch	ResNet9
batch_size	128
epochs	[5,10,15]
lrs	[0.001,0.0001,0.00001]
opt	["Adam","Adam","Adam"]

rates define how quickly the neural network updates the concepts it has learned by a value of step size. Lastly, the optimizers are algorithms that change attributes of the network such as learning rates to reduce error. Table 1 shows the model's hyperparameters as follows: ResNet9 model architecture, 128 image batch size, epochs [5, 10, 15], learning rate [0.001, 0.0001, 0.00001], and the Adam optimizer. This optimization algorithm was chosen because it can handle complex problems with noisy images, referring to blurry and grainy photos. After training the model, the validation set was loaded into the ResNet9 model and PM2.5 levels were analyzed solely from the images. The PM2.5 level predictions from the images were compared to the target PM2.5 levels that corresponded to the location and time of each image, which determined the accuracy of the model.

Results

After running the ResNet9 algorithm through the training dataset of 776 images from Beijing and Yosemite National Park (90% of the entire dataset) and the validation dataset of the remaining 86 images (10% of the entire dataset), the model yielded values of validation accuracy, training loss, and validation loss. Validation accuracy refers to the number of correct predictions obtained in the validation set. Training loss indicates the ResNet9 model's performance on fitting the training data. Validation loss indicates how well the model fits new data from the validation data to evaluate its performance. Figure 5 shows the relationship between the number of epochs used and the accuracy of the ResNet9 model. The graph reveals the model achieved an average accuracy of about 0.83 after roughly 15 epochs were run, which leveled out and remained consistent approaching 30 epochs. In Figure 6, the model's training loss

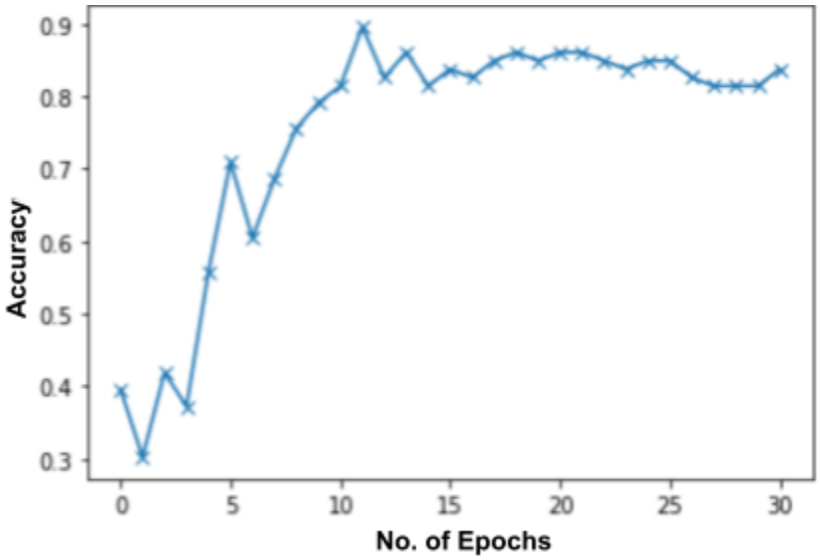

Figure 5: The effect of No. of Epochs on ResNet9 model accuracy
This graph displays the relationship between number of epochs used and accuracy of the ResNet9 model. Epochs refer to the number of times the learning algorithm runs through the entire training dataset. As epochs increase to 30, the accuracy levels out at a constant accuracy rate of roughly 0.83.

is averaged at 0.38, while its validation loss is approximately 0.42 after 30 epochs. Figure 6 shows both training and validation loss decreasing and stabilizing at a certain point, demonstrating a relatively optimal fit. However, the training loss is very slightly lower than the validation loss, indicating that there may be slight overfitting. Overfitting occurs when the validation loss is greater than the training loss, resulting in a model that cannot be generalized to new data. The model fits too well against the training

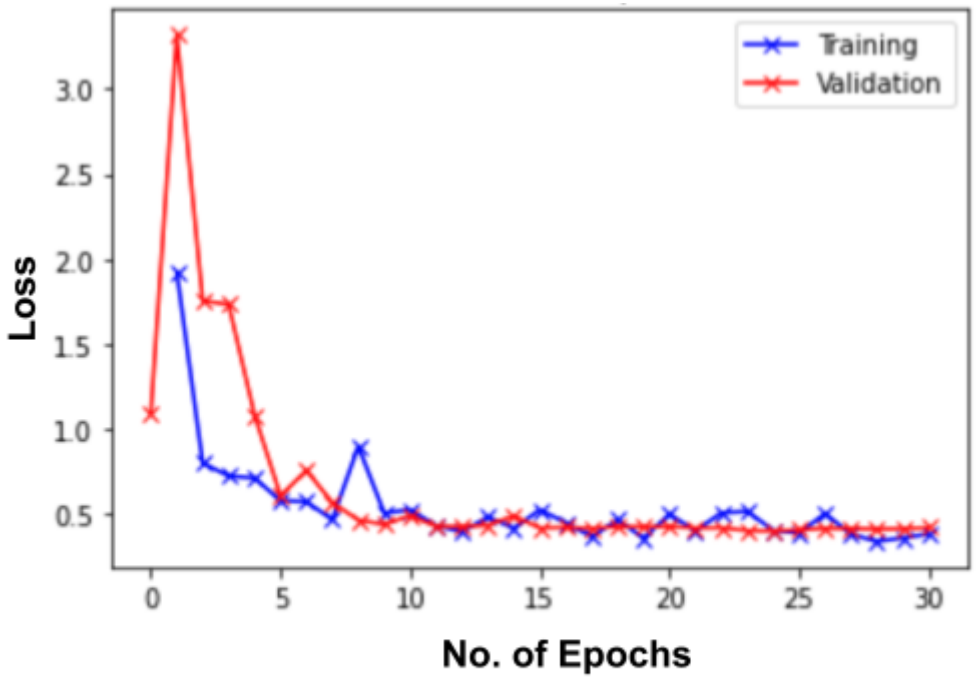

Figure 6: The effect of No. of Epochs on Training and Validation Loss This graph shows both training and validation loss decreasing to 0.38 and 0.42 respectively when 30 epochs are run on the ResNet9 model.

data and becomes not applicable to other data, such as the validation data. To prevent overfitting, training can be stopped early when the loss is low and stable.

Table 2: Table of metrics after training and testing the combined dataset from Beijing and Yosemite National Park, only Beijing, and only Yosemite National Park.

	Average Validation Accuracy	Average Training Loss	Average Validation Loss
Combined Dataset: Beijing and Yosemite National Park	0.83	0.38	0.42
Beijing Dataset	0.73	0.41	0.53
Yosemite National Park Dataset	0.97	0.06	0.11

In addition to training and testing the combined dataset of both Beijing and Yosemite National Park, metrics of validation accuracy, training loss, and validation loss were obtained from only the Beijing dataset and only the Yosemite National Park dataset. In both datasets that were run independently, hyperparameters remained the same, and images were classified into the same three categories of PM2.5 concentrations: Good (<35.4μg/m³), Unhealthy (35.5~150.4μg/m³), and Hazardous (>150.5μg/m³). 456 Beijing images were split into a training set of 411 images and a validation set of 45 images. 406 Yosemite National Park images were split into training and validation sets of 366 and 40 images respectively. These comparison values helped distinguish the causes of increased model performance from previous models: ResNet9 architecture was better suited for this problem or the larger and more diverse image dataset contributed to better generalization and therefore better performance of the model. As seen in Table 2, when the ResNet9 model was trained and tested on only the Beijing dataset, the average validation accuracy, training loss, and validation loss were 0.73, 0.41, and 0.53 respectively. Similarly, the Yosemite National Park dataset yielded average values of validation accuracy, training loss, and validation loss as 0.97, 0.06, and 0.11 respectively, when the model was trained and tested on only this particular dataset.

Figure 7: Comparison between webcam images obtained from Yosemite National Park (top) and Beijing (bottom). There are clear distinctions between geographic/scenic variations -- Beijing has more diverse images than Yosemite National Park.

Figure 7 shows a comparison between the Yosemite National Park (top) and Beijing (bottom) images. It is observable that Beijing has images from different webcams with diverse urban scenery, while Yosemite National Park images are from one webcam overlooking the same rural region: the Turtleback Dome. This distinction is prevalent and greatly influences the metrics generated from the training and validation sets.

Discussion

Analysis

As illustrated in Figure 5 and Figure 6, training the ResNet9 model with 30 epochs demonstrated optimal performance regarding accuracy and loss rates. Therefore, the model was able to successfully classify the Beijing and Yosemite National Park images into their respective PM2.5 levels with an average accuracy of approximately 83%.

Chakma *et al.* developed and tested a CNN model and Random Forest Classifier to detect PM2.5 levels in 591 real-time photos from the Beijing tourist website. Similarly, the CNN model classified the images into three categories: Good, Moderate, and Severe. After evaluating both methods of classification with randomly split training and validation sets, the CNN achieved an average accuracy of 68.74% and the Random Forest Classifier performed with an average accuracy of 63.62%.

After training and testing 456 images from the same Beijing tourist website, the ResNet9 model achieved an average accuracy of 73%, proving the ResNet9 architecture is better suited for this method of estimating PM2.5 concentrations over deep learning methods such as CNNs and Random Forest Classifiers. Further, by using a combined dataset of 862 images from two different locations, Beijing and Yosemite National Park, the ResNet9 algorithm had more training data to learn from, resulting in better performance than previous studies with smaller datasets. Training and testing on the combined dataset, the ResNet9 model achieved 83% average validation accuracy while the CNN and Random Forest Classifier achieved 68.74% and 63.62% respectively. Additionally, using two distinct regions with drastically different geographical features (urban and rural) allowed for greater generalization and applicability of the model in various areas globally.

When training and testing the Yosemite National Park dataset, the average validation accuracy rate was the highest out of the three datasets and the loss rates, or errors, were the lowest (Table 2). This is likely due to the simplicity of the images in this dataset, as seen in Figure 7. The 406 Yosemite National Park images were all taken from one webcam (NPS Turtleback Dome webcam), whereas the Beijing dataset obtained images from various webcams, therefore providing greater variability in images. Greater diversity in images allow for better generalization of the model when applied to different webcams. On the other hand, it is more difficult to achieve high accuracy rates on relatively small datasets. The Yosemite National Park dataset achieved a high average accuracy of 97%, and minimal errors from training loss of 6% and validation loss of 11%, because the images were relatively easy and simple to analyze. Therefore, the ResNet9 model is extremely applicable to singular webcams with limited variability, but requires large dataset training to be generalized to other locations with different geographic/scenic features.

Applications

The ResNet9 model has the potential to become an efficient and cost-effective monitoring method that would replace current monitoring systems that are broken and outdated. In areas where monitors don't exist altogether, this model can be easily implemented in comparison to current sophisticated air quality monitors.

An increase in monitoring will allow for the safety and protection of humans and our surrounding environment. Particularly in locations where landscapes and wildlife are emphasized and showcased, such as national parks, reducing air pollution is essential for the preservation of these areas. Monitoring systems will help improve air quality by allowing researchers to use collected data from these monitors to analyze air quality trends over time. Additionally, the ResNet9 model can intake large quantities of images -- for example, from webcams -- and allow researchers to closely examine changes in air quality between locations and timeframes.

Ultimately, the monitoring of air quality will most greatly benefit the human condition. When air quality is poor, humans become susceptible to a multitude of diseases, especially sensitive individuals such as children, older adults, or people with heart and respiratory ailments. Since pollution tends to build up in locations where there may be contributing sources of emissions and waste or are known to have weather conditions that decrease air quality levels, monitoring the pollution levels is crucial in informing governments and organizations to establish policies to control air pollution.

By potentially integrating the ResNet9 algorithm into a smartphone app, users will gain an even simpler method of monitoring air quality. Individuals can take a snapshot of their environment using their smartphone camera, and the algorithm will output an air quality metric (PM2.5, PM10, or ozone) in correspondence to the inputted photo. The algorithm consisting of neural network layers will break down each image into a precise pixelated form to better understand and classify each image in ways that the human eye is incapable of. This proposed app will allow day-to-day travelers to take precautionary measures, such as wearing a mask or avoiding places with an omnipresence of air pollution, to protect themselves from inhaling airborne particles, like PM2.5. They can also implement personal practices to reduce emissions, such as walking or biking rather than operating a gas-powered vehicle. An increase in accessibility to air quality monitoring will correlate with an increase in awareness among larger organizations and humans in everyday life to protect our health and the environment.

Future Research

Larger image and PM2.5 datasets from various geographic regions must be obtained to allow the training algorithm to learn and become more generalized with different locations. Moreover, apart from ResNet9, other CNN models can be tested to further improve classification accuracy.

Involving other variables such as precipitation, humidity, and temperature, can expand upon the image classification model and incorporate a unique aspect of air quality prediction into the future. By analyzing trends in weather, the model could potentially generate predictions of PM2.5 levels in the coming days or weeks, similar to a weather forecast. This research would be immensely beneficial to human and environmental health, especially in locations where air pollution levels are constantly fluctuating.

Conclusion

In this research, a ResNet9 model is introduced that can estimate levels of PM2.5 in images taken from Beijing and Yosemite National Park. The weather images were assigned and classified into three levels of PM2.5 concentrations: Good (<35.4μg/m³), Unhealthy (35.5~150.4μg/m³), and Hazardous (>150.5μg/m³). After training and testing on the validation set, the model demonstrated optimal performance results, indicating the ResNet9 model is a valid method of estimating levels of PM2.5.

Furthermore, a PM2.5 concentration image dataset was created with 862 images from webcams and the corresponding values of PM2.5 assigned to each image's date and location in Beijing and Yosemite National Park. Future research includes expanding this dataset to more geographic regions to increase the model's accuracy and applicability to various locations. Additionally, PM2.5 concentration forecasting using weather variables would be extremely useful for researchers and all humans. The developed ResNet9 model can decrease costs and increase the implementation of monitoring systems, which will improve the human condition by motivating people to engage in reducing air pollution and push governments to establish air quality monitors.

References

Alzubaidi, L., Zhang, J., Humaidi, A. J., Duan, Y., Santamaría, J., Fadhel, M. A., & Farhan, L. (2021). Review of deep learning: concepts, CNN architectures, challenges, applications, future directions. Journal of Big Data, 8(1), 1-74. https://doi.org/10.1186/s40537-021-00444-8

Chakma, A., Vizena, B., Cao, T., Lin, J., & Zhang, J. (2017). Image-based air quality analysis using deep convolutional neural network. 2017 IEEE International Conference on Image Processing (ICIP). https://doi.org/10.1109/icip.2017.8297023

Chen, C.-M., Lin, Y.-L., & Hsu, C.-L. (2017). Does air pollution drive away tourists? A case study of the sun moon lake national scenic area, Taiwan. Transportation Research Part D: Transport and Environment, 53, 398–402. https://doi.org/10.1016/j.trd.2017.04.028

Chenthamarakshan, V., Das, P., Hoffman, S. C., Strobelt, H., & Padhi, I. (2020, June 24). CogMol: Target-Specific and Selective Drug Design for COVID-19 Using Deep Generative Models. Cornell University. Retrieved December 3, 2021, from https://arxiv.org/abs/2004.01215

Eusébio, C., João Carneiro, M., & Madaleno, M. (2021). The impact of air quality on tourism: a systematic literature review. Journal of Tourism Futures, 7(1).

Friedman, C., Hripcsak, G., & Shablinsky, I. (1998). An evaluation of natural language processing methodologies. Proceedings. AMIA Symposium, 855–859.

He, K., Zhang, X., Ren, S., & Sun, J. (2015). Deep Residual Learning for Image Recognition. arXiv. https://doi.org/10.48550/arXiv.1512.03385

Keiser, D., Lade, G., & Rudik, I. (2018). Air pollution and visitation at U.S. national parks. Science Advances, 4(7). https://doi.org/10.1126/sciadv.aat1613

Kortoçi, P., Motlagh, N. H., Zaidan, M. A., Fung, P. L., Varjonen, S., Rebeiro-Hargrave, A., Niemi, J. V., Nurmi, P., Hussein, T., Petäjä, T., Kulmala, M., & Tarkoma, S. (2022). Air pollution exposure monitoring using portable low-cost air quality sensors. Smart Health, 23, 100241. https://doi.org/10.1016/j.smhl.2021.100241

Koutsoukas, A., Monaghan, K. J., Li, X., & Huan, J. (2017). Deep-learning: Investigating deep neural networks hyper-parameters and comparison of performance to shallow methods for modeling bioactivity data. Journal of Cheminformatics, 9(1). https://doi.org/10.1186/s13321-017-0226-y

Lenzen, M., Sun, Y.-Y., Faturay, F., Ting, Y.-P., Geschke, A., & Malik, A. (2018). The carbon footprint of Global Tourism. Nature Climate Change, 8(6), 522–528. https://doi.org/10.1038/s41558-018-0141-x

Maille, B., Wilkin, M., Million, M., Rességuier, N., Franceschi, F., Koutbi-franceschi, L., Hourdain, J., Martinez, E., Zabern, M., Gardella, C., Tissot-dupont, H., Singh, J. P., Deharo, J.-C., &

Fiorina, L. (2021). Smartwatch electrocardiogram and artificial intelligence for assessing cardiac-rhythm safety of drug therapy in the covid-19 pandemic. the qt-logs study. International Journal of Cardiology, 331, 333-339. https://doi.org/10.1016/j.ijcard.2021.01.002

McCarthy, G., & Burke, T. A. (2017, May). We need a strong Environmental Protection Agency: It's about public health! American journal of public health. Retrieved September 27, 2022, from https://www.ncbi.nlm.nih.gov/pmc/articles/PMC5388973/

Rachmatullah, M., Santoso, J., & Surendro, K. (2021). Determining the number of hidden layer and hidden neuron of neural network for wind speed prediction. *PeerJ. Computer Science*, *7*, e724. https://doi.org/10.7717/peerj-cs.724

Rajakariar, K., Koshy, A. N., Sajeev, J. K., Nair, S., Roberts, L., & Teh, A. W. (2020). Accuracy of a smartwatch based single-lead electrocardiogram device in detection of atrial fibrillation. Heart, 106(9), 665-670. https://doi.org/10.1136/heartjnl-2019-316004

Sadiq, A. S., Faris, H., Al-Zoubi, A. M., Mirjalili, S., & Ghafoor, K. Z. (2019). Fraud detection model based on multi-verse features extraction approach for Smart City Applications. Smart Cities Cybersecurity and Privacy, 241–251. https://doi.org/10.1016/b978-0-12-815032-0.00017-2

Xing, Y. F., Xu, Y. H., Shi, M. H., & Lian, Y. X. (2016). The impact of PM2.5 on the human respiratory system. , (1), E69–E74. https://doi.org/10.3978/j.issn.2072-1439.2016.01.19

Xing1, Y., & Li1, F. (2020, April 1). Research on the influence of hidden layers on the prediction accuracy of GA-BP neural network. Journal of Physics: Conference Series. Retrieved September 27, 2022, from https://iopscience.iop.org/article/10.1088/1742-6596/1486/2/022010

Zhuang, F., Qi, Z., & Duan, K. (2020). A Comprehensive Survey on Transfer Learning. https://doi.org/https://doi.org/10.48550/arXiv.1911.02685